Safety assessment of the Torre de la Vela in la Alhambra, Granada, Spain: The role of on site works

Annalaura Vuoto [a,*], Javier Ortega [a,b], Paulo B. Lourenço [a], Francisco Javier Suárez [c], Antonieta Claudia Núñez [d]

[a] ISISE, Department of Civil Engineering, University of Minho, Guimarães, Campus de Azurém, 4800-058 Guimarães, Portugal
[b] Instituto de Tecnologías Físicas y de la Información (ITEFI) Leonardo Torres Quevedo, Consejo Superior de Investigaciones Científicas (CSIC), C/Serrano 144, 28006 Madrid, Spain
[c] Universidad de Granada, Departamento de Mecánica de Estructuras e Ingeniería Hidráulica, Campus Universitario de Fuentenueva (Edificio Politécnico), 18071 Granada, España
[d] PROSKENE Conservation & Cultural Heritage, Calle Santa Engracia 108, 7 ext. dcha., 28003 Madrid, España

ARTICLE INFO

ABSTRACT

The Alhambra is a UNESCO World Heritage Site located in Granada, which is the area with the highest seismic hazard in Spain. The present work focuses on the seismic safety evaluation of the *Torre de la Vela*, the main tower of the *Alcazaba*, the fortress of the Alhambra and the first area of the citadel built in the 13th century. The safety evaluation is carried out using finite element modeling and nonlinear static analyses. In a first phase, a numerical model of the tower was prepared based solely on bibliographic review and a first set of analyses was carried out. In a second phase, the monument was visited and a detailed survey including non-destructive testing was carried out. A second set of analyses was performed using an updated model calibrated with experimental results and the seismic safety assessment was carried out. The results are systematically compared and highlight the importance of on-site works for a correct safety assessment of historic structures.

1. Introduction

Built cultural heritage constitutes a landmark providing identity to cultures, regions and towns. Moreover, historical constructions are a live document providing outstanding cultural and technical achievements related to a specific historical period or to a population [1]. These aspects particularly define the Alhambra of Granada, located in southern Spain. The Alhambra is a UNESCO World Heritage Site from 1984 and one of Spain's major attractions. The complex was begun in 1238 by Muhammad I Ibn al-Ahmar, the first Nasrid emir and founder of the Emirate of Granada, the last Muslim state of Al-Andalus. It bears exceptional testimony to the Muslim Spain of Al-Andalus between the 13th and 15th centuries. The complex is highly enriched by the symbolic value held by the different parts, which, since the 13th century, have been mostly preserved in their original configuration.

As it is generally acknowledged, the current concept of monument can include groups of separate or connected buildings which, because of their architecture, homogeneity or place in the landscape, are of outstanding universal value from the historical, artistic or technical point of view [1,2]. This concept perfectly reflects the value of the Alhambra as cultural heritage. For such a type of monumental complex, it is crucial to preserve all its parts, which are essential for the overall understanding of the monument. In this perspective, the present work is focused on the structural safety evaluation of the *Torre de la Vela*, the main tower of the *Alcazaba*, fortress of the Alhambra and first area of the citadel to be built in 13th century.

Structural analysis plays an important role in the diagnosis and the safety evaluation of historic buildings, because it allows to obtain quantitative predictions on the response of the building when subjected to different actions. Structural analysis becomes an essential tool when it comes to masonry buildings in seismic areas, as in the case of Granada, which is characterized by the highest level of seismic hazard in Spain.

The structural safety assessment of the *Torre de la Vela* is carried out by using finite element modelling and non-linear static analysis, which allowed to understand its structural behavior and seismic resisting mechanisms. In the first phase of the work, the preparation of the

numerical model was entirely based on data collected from the available literature, given the pandemic situation of recent times. A thorough bibliographic review was of fundamental importance for the understanding of the geometric, material and structural characteristics of the building. In the second phase, a comprehensive *in-situ* experimental campaign was conducted in order to characterize the main structural aspects and update the preliminary numerical model. The work included a detailed geometric survey of the tower, using laser scanner, sonic tests to characterize the tower's materials properties and dynamic identification test to characterize the global structural behavior of the tower.

The comparison of the results of the structural analyses performed before and after the *in-situ* investigations highlights the importance of the latter for a correct evaluation of the structural safety of historic buildings, which is the major contribution of the present study. In fact, the introduction of information deduced from experimental data in the numerical models can lead to outcomes that may be significantly different from the hypotheses formulated solely on the basis of literature and historical documentation. This further stress the adequacy of modern assessment standards, which consider explicitly the level of knowledge in the safety assessment as a way to consider uncertainty regarding geometry, detailing (or internal morphology and structural details) and material data.

1.1. Torre de la Vela in the context of the Alhambra

The Alhambra was built during the so-called Hispano-Muslim Middle Ages, between the 13th and 14th centuries, and played many different roles as palatine city, Christian Royal House, General Captaincy of the Kingdom of Granada and military fortress, until its declaration as a National Monument in 1870. It sits on the hill that the Arabs called al-Sabika (Fig. 1 (above)), which is located on the left bank of the Darro River and elevated to the East of the city (790 m above sea level). Undoubtedly, there were buildings before the Muslim domination due to the strategic location of the site, which were rebuilt in the Arab period, often becoming a shelter and refuge for the population. The enclosure of the Alhambra, called *Alcazaba* (highlighted in red in Fig. 1 (below)), was scene of confrontations in the civil wars of the Caliphate of Córdoba, often being a refuge for warlords, who made repairs, gradually widening.

When the Kingdom of Granada was constituted in the 13th century under the Nasrid dynasty, its founder, Muhammad b. al-Ahmar, decided to establish his residence at the Alhambra and to join his palace to the existing fortress. This was the beginning of the Alhambra's period of splendor. Al-Ahmar rebuilt and reinforced the old part of the *Alcazaba*, personally directing the works, building then among others the *Torre de la Vela* and the *Torre del Homenaje* [3].

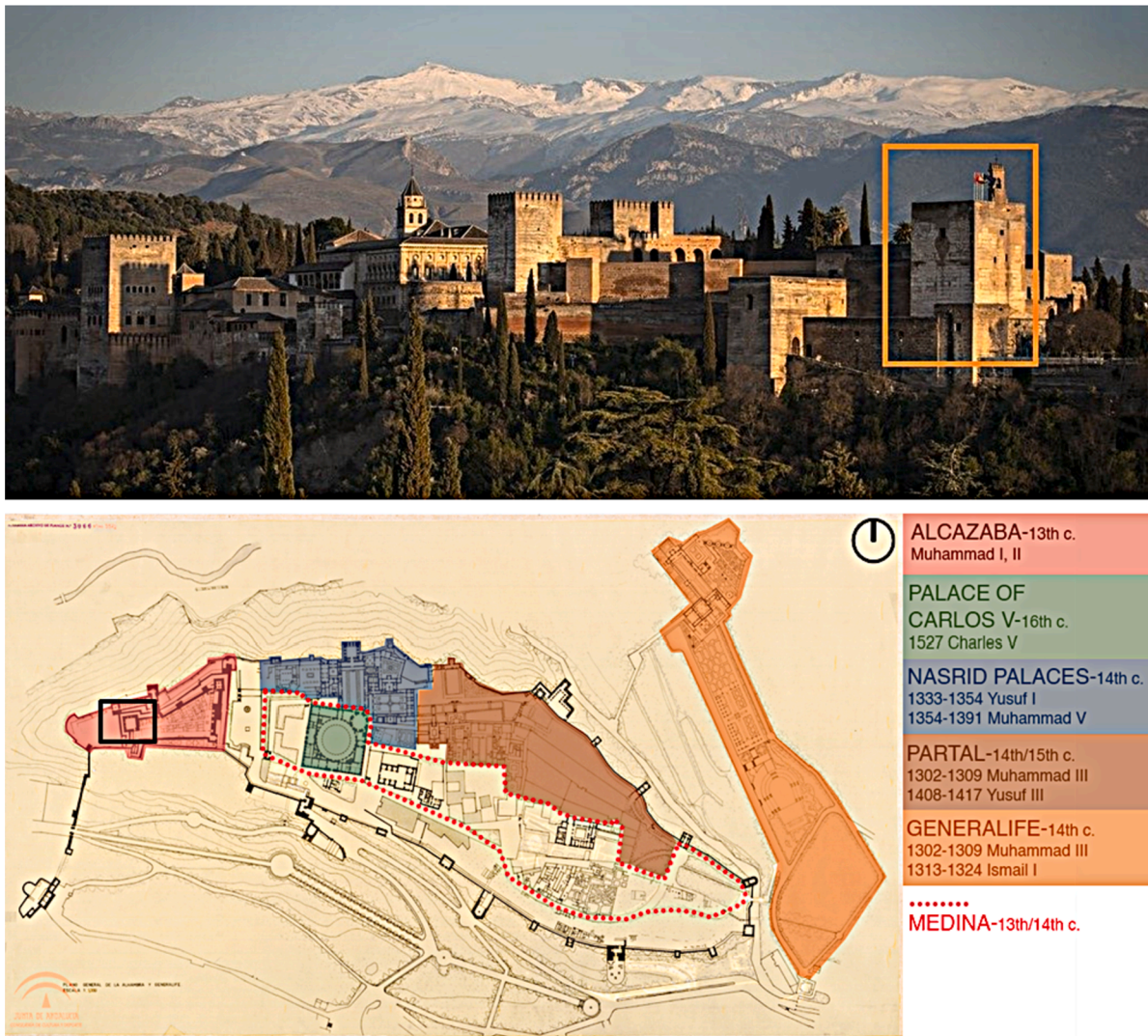

Fig. 1. (above) North elevation of the Alhambra with the *Torre de la Vela* highlighted; (below) Plan of the Alhambra, the different areas of the complex and their period of construction are shown. Torre de la Vela is marked in black square.

After the Granada war and the end of the Nasrid dynasty, in 1492, the Catholic Monarchs appointed the *Conde de Tendilla* as governor of the Alhambra. They built new access roads, and repaired towers and walls, using for this purpose the *farda* tax levied on the subjugated people.

On the 16th century and on the occasion of their wedding, Emperor Carlos V and Isabel de Portugal traveled to the Alhambra, which involved a major set of reforms and the construction of the splendid Renaissance palace [4].

With the arrival of the 18th century, King Philip V removes from the governorship of the Alhambra, the *Marqueses de Mondejar*, descendants of the *Condes de Tendilla*, for having supported the party of the Austrian archduke in the War of Succession. The Alhambra begins a period of total abandonment, becoming a place for vagrants and being the object of thefts and damage. During the Napoleonic invasion, the Alhambra was used as barracks to house French troops, who blew up part of the fortress when they abandoned it in 1812.

The Alhambra was in danger of disappearing, being saved by the interest it aroused in the romantic travelers of the 19th century, who spread a new orientalist vision of the monument that enhanced its consideration in emotional terms. The best known among these travelers is the American Washington Irving [4–6].

After the 1868 revolution, the Alhambra went from being a Royal property to a monument of the Nation. In 1870, it was declared a national monument, and a fixed amount was allocated in the national budget for conservation works. Since then, maintenance activities have developed increasingly, highlighting the work of important architects such as Leopoldo Torres Balbás, who, at the beginning of the 20th century, established the basis for the conservation of the Alhambra.

In 1943, the enclosure was catalogued as a historic garden. In 1984, UNESCO declared the Alhambra and the Generalife a World Heritage Site.

In the *Torre de la Vela*, and in in the set of the towers of the *Alcazaba*, we can perceive the constructive traditions of Almohad military architecture, which incorporated to the old defensive structures of the Spanish caliphal and *taifa* tradition, new artifices arrived through the Mediterranean, coming from the architecture of Byzantine fortifications. It is an architecture of great sobriety and constructive sense [7], combining elements of exaggerated dimensions with vaults and elements of palatine architecture.

The *Torre de la Vela* received its name in Christian times, in homage to the first bell called *La Vela*, which was installed to announce the conquest of the city in 1492 and was used for many years to alert the population about events such as robberies, riots or fires. The bell is nowadays a symbol of the city of Granada [3].

The *Torre de la Vela* is therefore one of the longest-standing buildings of the entire Alhambra. It is a feudal-style tower of residence [8] that, throughout the centuries, has undergone numerous conservation and repair works, as well as to alterations in its interior configuration. The alterations were a consequence of many natural and historical events, such as the earthquake of 1522, a gunpowder explosion in the Darro Valley in 1590, or a lightning strike in 1882, which destroyed the wall of the pediment where the bell was initially located [9]. Some of the alterations are evident from the outside, such as the missing battlements of the terrace and the areas repaired with brick masonry of a different texture than the original rammed earth walls. With regard to the latter, the presence of cracks in the facades should be noted. However, these do not seem to be due to structural phenomena but rather to the coexistence of the two materials, which showed different behavior.

With respect to the geological characteristics, the Alhambra was constructed on a conglomeratic sequence that constitutes the so called *formación Alhambra* (Alhambra formation). This soil is composed by a clay matrix with different size limestone particles. The ground is classified Type D according to Eurocode 8 [10]. The monument is in a peculiar area from the tectonic point of view: the al-Sabika hill dominates a plain, surrounded by mountains, where most of the city of

Granada extends. This depression is located in the central sector of the Betic Cordillera, and is one of the most seismically active zones in the Iberian Peninsula [11].

2. Preliminary current state assessment of the *Torre de la Vela*

A preliminary assessment of the current state of the tower was achieved through a comprehensive study of the literature [12–17], on the basis of which a numerical model was prepared (Section 2.3) and used to carry out non-linear static analyses for vertical and horizontal loads. The preliminary numerical analysis is presented in Section 2.4. The results of this analysis are further compared in Section 4.3 with the results of the same analysis conducted on the updated model.

The historical drawings (plans and one cross section) belonging to the studies by Gómez Moreno [12] (prior to 1907) and López Bueno (between 1923 and 1936) [13] were used as the main reference for the construction of the geometrical 3D model, supported by a detailed description of the geometry of the tower provided by Pavón [14] and Gómez Moreno [12]. The assessment of the geometrical configuration is presented in Section 2.1. In addition, the available information on traditional construction techniques and materials is reported in Section 2.2, based on which the mechanical properties adopted for the structural model have been defined. For the characterization of the materials in the *Torre de la Vela*, reference is made to the study of the *Torre del Homenaje*, another tower of the *Alcazaba*, carried out by Villegas [15], which in turn refers to different sources, both experimental and normative. The *Torre del Homenaje* and the *Torre de la Vela* date back to the same period and their constructive system is similar. Therefore, it was considered plausible to use the same characterization.

2.1. Geometry

Located in the western border of the *Alcazaba* fortress, the *Torre de la Vela* is its highest tower, with a height of 26,80 m. It is a squared tower with 16 m side plan, divided into four floors and a terrace top floor with the bell gable. The ground floor of the tower (Floor 1 in Fig. 2 (left)) is a sort of single nave dungeon with rectangular plan. The three upper floors (Floor 2, 3, and 4 in Fig. 2 (left)) show the same layout, with a squared central area enclosed by two naves on the four sides. The width of the outermost nave increases from the second to the last floor plan, as the outer wall decreases in thickness, from 4,60 m in the ground floor to 1,62 m in the last floor [12].

Analyzing the plans' arrangement, it appears that the correspondence of pillars and internal walls between the second floor and the remaining ones was not guaranteed. This caused deformations in the vaults, cracks and crushing of the pillars at the second floor. Therefore, two arches and a wall were added in the central room of the first floor and many openings were closed in the others. However, the damage increased again due to the 1522 earthquake, according to a coeval document, and probably became even worse because of the blast of gunpowder in 1590. Some parts were rebuilt, the closing of arches on the second and third floors continued, causing the loss of the original configuration. A modern staircase was added when the top floor was converted into an apartment [8].

The internal layout, with naves in the central part and arches in the corners, is a typical byzantine solution incorporated into Muslim architecture since the 10th century. The arches are almost all horseshoe-shaped. There are segmental arches in the last floor and two pointed arches in the first floor, unique examples in the whole *Alhambra*. The vaults are of different type and have complex configurations, especially the ones covering the central square of each floor (Fig. 2 (right)).

The layout was simplified to prepare the geometrical model. The layout assumed for the 3D model was defined as follows (see Fig. 3): 1 - central square open with a variable number of arches; 2 - external square, which encloses the inner narrow nave, open with a variable number of arches; 3 - walls bracing the corners of the outermost nave
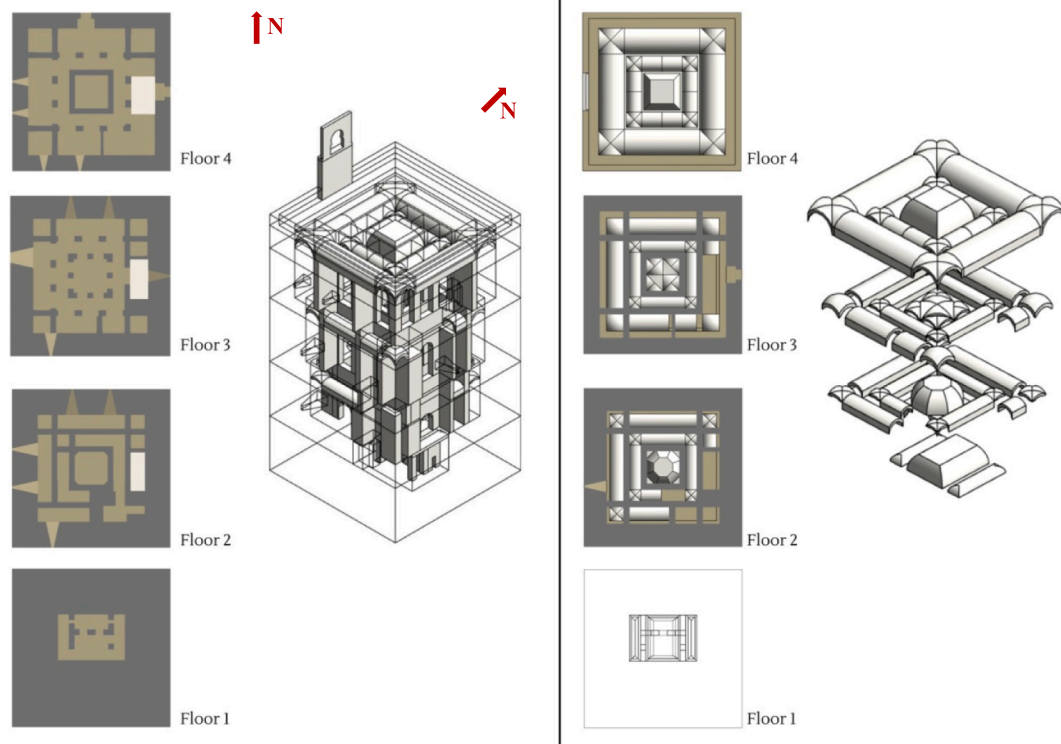
Fig. 2. (left) Reconstruction of plans and 3D model; (right) vaults layout; according to existing drawings and literature.

(according to the available description [12], these walls were originally arches, some of which are closed. Given the lack of detailed information, walls have been modelled without openings); 4 - vaults of variable typology; 5 - vaults' infill; 6 - external walls.

2.2. Construction techniques and material properties

In the Alhambra, rammed earth and brick masonry are widely used for towers, gates and city walls. Originally, the external walls of the towers were built in rammed earth, meaning that it is possible to locate the reconstructed parts in brick masonry, with a simple visual inspection. Bricks are widely used in the internal structures of the towers, to build pillars, arches, vaults, staircases and, in general, in all parts where a better structural behavior was required or where an ornament was to be introduced [8].

Two main references have been used for the understanding of material properties and construction techniques found in the *Alhambra*. The first one is a study carried out by de la Torre López [16], which assesses the chemical, mineralogical, petrographic and textural characteristics of rammed earth by several experimental laboratory tests. The other is a comprehensive study carried out by the Laboratory of Geotechnics of CEDEX (*Centro de Estudios y Experimentación de Obras Públicas*), which focused on the characterization of the *Torre de Comares* [18].

2.2.1. Traditional construction techniques

The *Torre de la Vela*'s outer shell is made of rammed earth, showing some reconstructed areas made of clay brick masonry. The inner structural elements, pillars, arches and vaults, are made of well-baked irregular clay bricks assembled with mortar joints up to 3 cm thick. The employed mortar is loose and made of earth, clay and lime, except for the one used in the vaults, which is a hard gypsum mortar [12]. Plasterwork, when present, is made of lime mortar.

The earthen walls used in the Alhambra comprise the traditional method of construction for most of the outer walls in Hispano-Muslim grenadine architecture [16]. One particular type of rammed earthen wall found in the *Alcazaba* is the so-called *tapial calicostrado,* rich in sand

and lime. The outer walls of the *Torre de la Vela* are made with this technique. This type of earthen wall is not made of homogeneous material. Layers richer in clay (reddish) and richer lime (light-colored) were placed alternately into the formwork. As depicted in Fig. 4 (a), the lime layers were placed in the outer part of the wall arranged in wedges with the wide part forming the outer face. After compacting the whole, the layers of lime ended up forming a homogeneous surface on the outside of the wall. The outward appearance and the intermixing of the two earthen mixes (light-colored and reddish) seen under the microscope, seem to indicate that the two were erected and compacted simultaneously [16].

Despite the thickness of the rammed earth walls, there is no reasonable indication to consider them as double-leaf walls. This is easily understandable considering the markedly defensive character of the building. In addition, studies on contemporary defensive towers have assessed that the outer walls are continuous in height [18].

The brick units used for the inner structure of the *Torre de la Vela* have dimensions equal to $29 \times 14 \times 5\text{-}6$ cm and belong to the so-called *ladrillo Almohade* (Almohad brick) typology. The mortars used to assemble the brick units, with thick joints, are very similar, in their components, to the rammed earth. Most of the materials employed both for rammed earth walls and mortars come from the local soil, the above mentioned *formación Alhambra*, because of the proximity and availability of the material.

Based on available references [19–22], the information collected for other towers of the *Alcazaba* dating back to the same period, and several pictures, the layout proposed in Fig. 4 (b) is assumed for the *Torre de la Vela*.

2.2.2. Material properties

The rammed earth employed in the external walls of the *Torre de la Vela* can be considered homogeneous throughout the tower, with the exception of the aforementioned reconstruction of some parts carried out using brick masonry. Table 1 shows the mechanical properties obtained after the above mentioned experimental campaign carried out by CEDEX [15]. Attention should be paid to the differentiation between the
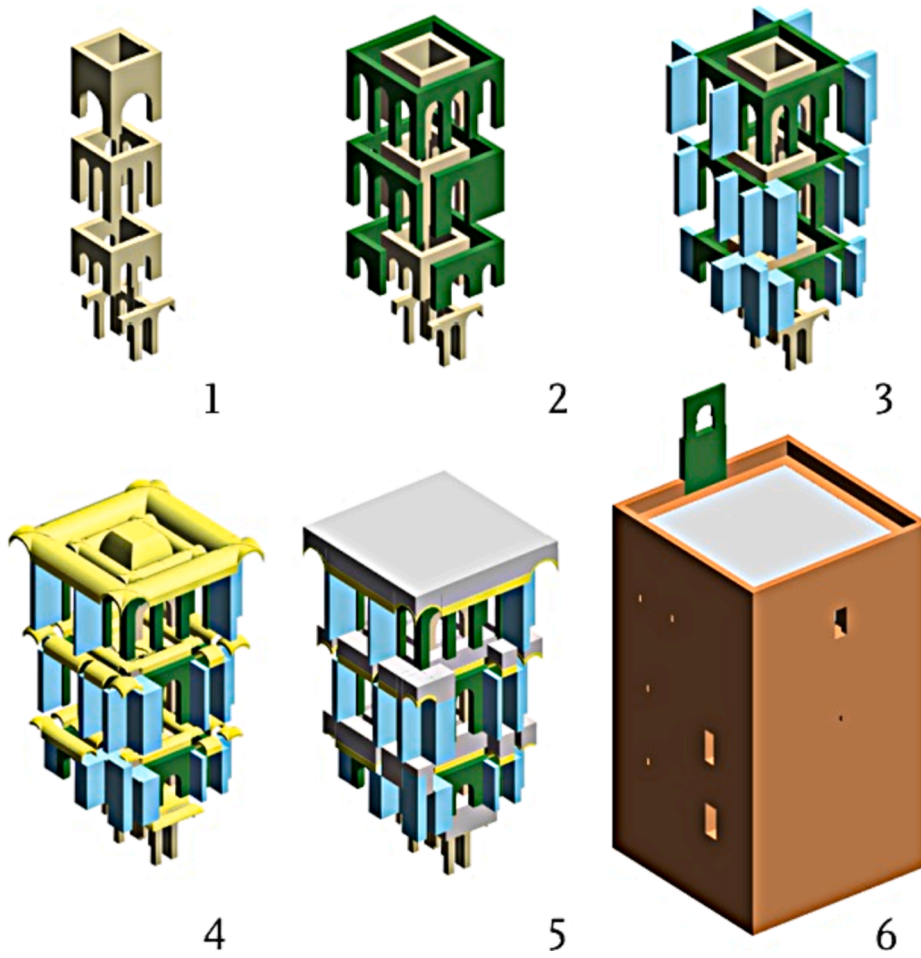
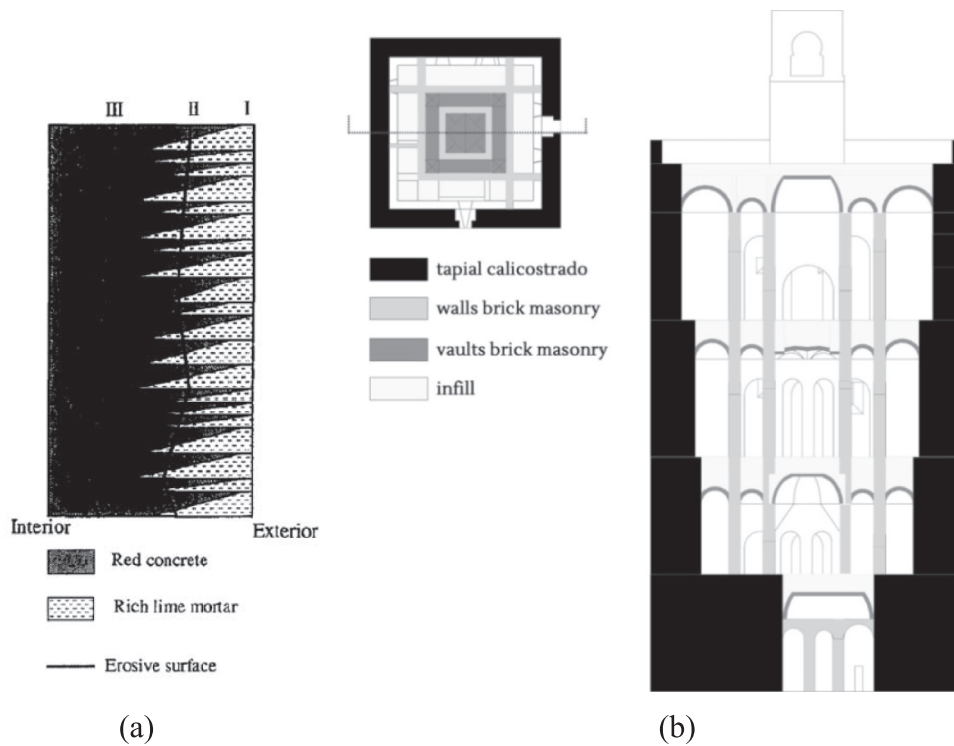**Fig. 3.** Layout assumed for the numerical model.

Fig. 4. (a) Layering of the *tapial calicostrado* wall, vertical cross section; (b) material and structural layout assumed for the *Torre de la Vela*.

Table 1

Mechanical properties of *tapial calicostrado* according to CEDEX experimental campaign [15].

Property	Value		Test Standard
Bulk density	2,250 kg/m^3		UNE 83.312-90
Compressive strength (f_c)	2.5 MPa	Structure	UNE 83.304-84
	8.0 MPa	Foundations	
Tensile strength (f_t)	0.30 MPa	Structure	UNE 83.306-85
	0.75 MPa (ratio 1/8 approximately)	Foundations	
Young's modulus (E)	1200 MPa	Structure	ASTM C-469-87
	6300 MPa (at 40% of ultimate strength)	Foundations	
Poisson's ratio (ν)	0.3	Structure	ASTM C-469-87
	0.2	Foundations	

rammed earth used for the foundations and the one used in the above-ground floors.

As regards the brick masonry, it is necessary to consider the different sources of heterogeneity and non-linearity of the material, as well as the lack of an experimental characterization. In fact, the study carried out by CEDEX only provides experimental data for the brick units, shown in Table 2, lacking information about the mortar and the masonry. For this reason, for the mechanical characterization of the masonry, reference was made to technical codes, as given in Section 2.3.

2.3. Preparation of the numerical model based on literature data

The numerical model of the *Torre de la Vela* was implemented in the software DIANA (DIsplacement ANAlyzer) FEA (Finite Element Analysis) (developed and distributed by DIANA FEA BV) [23] using literature data both in terms of geometry and mechanical properties of materials.

The numerical model was obtained by importing into DIANA FEA the geometric model previously built in Autocad 3D using solid elements. The numerical model is therefore composed of three-dimensional (3D) solid elements. These elements are, usually, the most adequate to model historical masonry structures, often characterized by massive elements. However, their use is usually time consuming, considering the time needed to prepare the model, perform the calculations, and analyze the results. Nevertheless, the description of 3D stress state is often inevitable for historical structures. Shell models (2.5D) consider only the middle plan of the element, while the rigid stiffness of the connection between two orthogonal elements is not considered. The connection stiffness is particularly important for the global response in the case of historical masonry structures, as the walls are generally very thick when compared to their length or height. On the other hand, plane stress models (2D) are often inapplicable to historical structures, given the intrinsic three-dimensional effects present. In a few cases, they can be used to analyze parts of the building [24].

While the external structure of the tower is very simple, the interior is complexly articulated. Thus, the intent was to preserve as much as possible the internal configuration in the structural model both to understand the influence of the inner elements on the overall behavior of the structure and because the greater concentration of damage was expected for these elements, (arches, vaults, pillars), theoretically more

Table 2

Mechanical properties of brick units according to CEDEX experimental campaign [15].

Property	Value	Test Standard
Bulk density	1,450 kg/m^3	UNE 67-019-86
Compressive strength	15.0 MPa	UNE 67.026-86

vulnerable than the massive external walls. For this reason, the geometrical model has a considerable number of different elements, resulting in 257 structural solid shapes.

Boundary conditions were set in DIANA. In the absence of specific data, fixed supports were assigned to the base of the structure. The foundation nodes were considered fixed against both translation and rotation in the three main directions, so the foundation was considered rigid. The presence of adjacent structures in the East and South façade was discarded at this step of the work. All elements of the numerical model were considered perfectly connected in the absence of more detailed information.

A fair compromise between accuracy and computational efforts was achieved for the mesh design of the *Torre de la Vela*. The mesh size was assigned as a function of the size of the element, with different size set from 0.5 m in the thick external walls to the 0.2 m in the vaults. The used mesh type is quadratic/hexagonal, except for some of the vaults for which the triangle/tetrahedron fitted better. The most recurrent element type is a five-node isoparametric solid pyramid element, with a five-point integration scheme over the volume. The other recurrent element type is an eight-node isoparametric solid brick element, with a $2 \times 2 \times 2$ integration scheme. The final model has 171,381 nodes and 290,113 elements (Fig. 5).

A macro-mechanical based finite element model was employed for the structural analysis of the Torre de la Vela. Three different materials were defined in DIANA according to the mechanical characterization discussed in Section 2.2.2 and assigned to the elements according to the discretization shown in Fig. 4. As stated in Section 2.2.2, for the assessment of the mechanical properties of brick masonry, several reference values provided by technical Codes were taken into account. In particular, reference was made to the Table C8.5.I provided by the Annex [25] to the Italian Building Code (Norme tecniche per le costruzioni DM17/01/2018 (NTC2018) [26]) and the values used by Villegas [15] for the Torre del Homenaje, which in turn were based on both the Eurocode 6 (EC-6) and the Spanish Code.

As regards the Italian Code, the values provided for masonry made in solid bricks and lime mortar are considered. The Table C8.5.I indicates the following minimum and maximum values for mechanical properties: compressive strength (f) = 2.6–4.3 N/mm^2, Young's Modulus (E) = 1200–1800 N/mm^2, Shear Modulus (G) = 400–600 N/mm^2, unit weight (w) = 18 kN/m^3. As regards the work by Villegas, the following average values were assessed with reference to both EC-6 and Spanish Code: compressive strength (f) = 4 N/mm^2, Young's Modulus (E) = 1600 N/mm^2, unit weight (w) = 14.50 kN/m^3. Therefore, according to the collected reference values, the bulk density is assumed equal to 1,600 kg/m^3, considering the experimental value obtained for the brick units (Table 2) increased by about 10% to take into account the presence of the mortar. The values of compressive strength (fc) and Young's Modulus (E) are within the ranges proposed by the Italian Code [25,26] and also aligned with those used by Villegas [15]. The tensile strength (ft) is assumed equal to 5% of the compressive strength.

The properties of the infill above arches and vaults are similar to those of the external rammed earth walls according to CEDEX report [17]. Therefore, following the approach of Villegas [15], the same bulk density is assumed, although with a much lower Young's Modulus, set equal to the 50% of the rammed earth one, considering the infill does not provide significant stiffness to the whole structure.

Linear and non-linear mechanical properties are listed in Table 3, where ρ is the specific mass, E is the Young's modulus, ν is the Poisson's ratio, f_c is the compressive strength, G_{fc} is the compressive fracture energy, f_t is the tensile strength, G_{ft} is the Mode-I tensile fracture energy. The compressive fracture energy was obtained using a ductility index d of 1.6 mm, which is the ratio between the fracture energy and the ultimate compressive strength [27]. The Mode I fracture energy (G_{ft}) was calculated according to the following formulation: $G_{ft} = 0.04 * f_t^{0.7}$ [28].
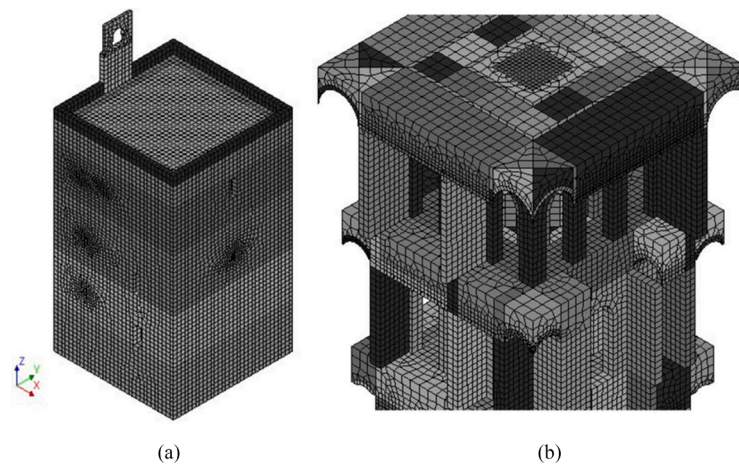
Fig. 5. Meshed model in DIANA FEA. (a) External view; (b) internal view.

Table 3
Material properties used in the analysis.

Material	Reference	E [MPa]	ν [-]	ρ [T/mm³]	f_c [MPa]	G_{fc} [N/mm]	f_t [MPa]	G_{ft} [N/mm]
Rammed earth	*Villegas*	1200	0.30	2.25E−09	2.5	4.0	0.3	0.017
Brick masonry	*Italian Code*	1600	0.25	1.60E−09	4.0	6.4	0.2	0.013
Infill	*Villegas*	600	0.30	2.25E−09	2.5	4.0	0.3	0.017

The non-linear behavior of the materials was described using a Total Strain-Based Crack Model (TSBC) with a rotating crack formulation [29,30]. The TSBC can describe both tensile and compressive behavior of a given material with one stress–strain relationship. An exponential function was considered for the tensile softening and a parabolic curve was assumed for compression.

2.4. Non-linear static analyses

For the analyses described in this section, a mechanical non-linearity was taken into account. The non-linear characterization of the materials is described in Section 2.3. An incremental vertical analysis was performed in order to understand the behavior of the building under its self-weight. Due to the characteristic of the tower, remarkably massive, it was considered not significant to perform the analysis until reaching the
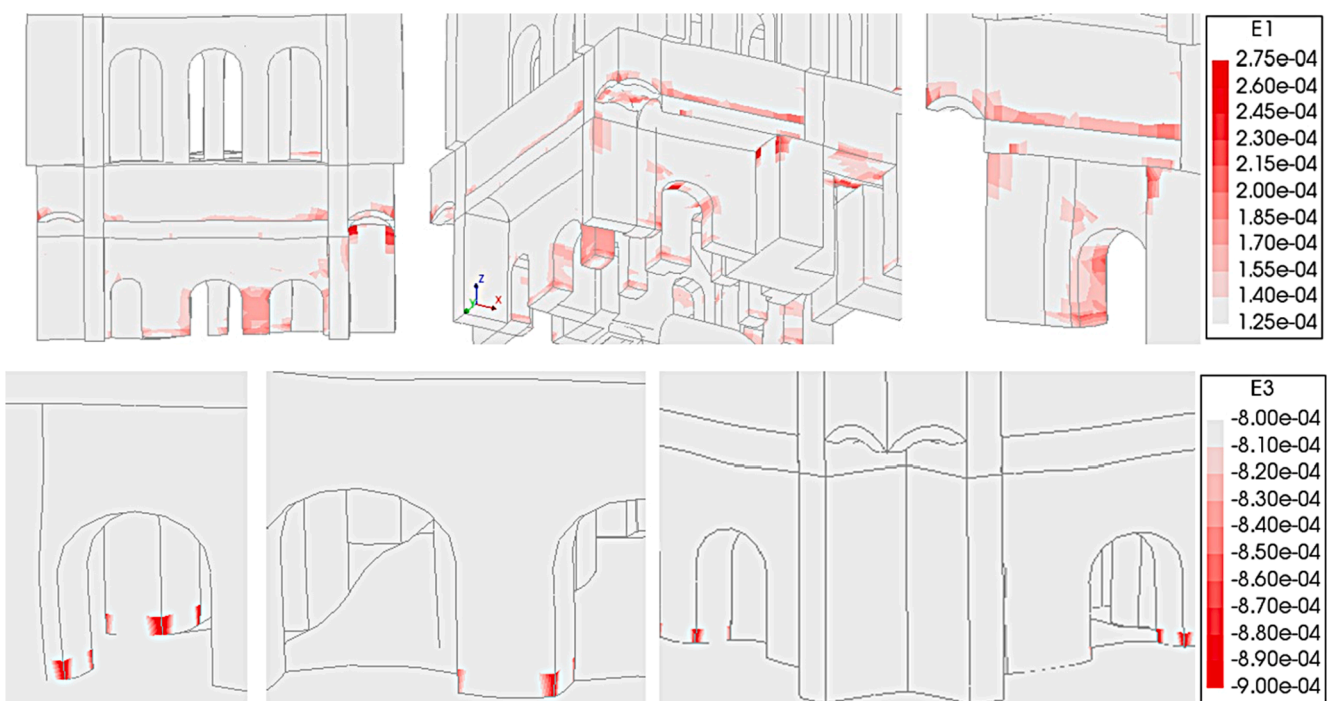

Fig. 6. (above) Maximum principal strain distribution in masonry structures above peak tensile strain (1.25E-4); (below) minimum principal strain distribution in masonry structures above elastic strain limit (8.33E-4).

maximum value of the vertical load. The main objective of the analysis was to investigate the response under the current vertical load, namely the self-weight. It was decided to push the analysis slightly beyond the application of a vertical load equal to the self-weight by doubling it through a Load Factor (LF) equal to 2. However, with this LF, the structure's overall behavior is basically still linear. The results in Fig. 6 are therefore shown for a LF equal to 1 (self-weight). Cracking is assessed analyzing values of maximum principal strain E1. Cracking appears above the peak strain (equal to 1.25E-4) at masonry elements. It is mainly observed at the pillars and arches of Floor 2, as shown in Fig. 6 (above) and in accordance with literature information regarding the arising of damage in this area of the tower. Crushing in the tower is assessed analyzing the values of minimum principal (compressive) strain (E3). As visible in Fig. 6 (below), localized crushing appears after reaching the elastic compressive strength ($f_c/3$ according to the used constitutive model, corresponding to an elastic strain limit equal to 8.33E-4), at several masonry pillars in Floor 2.

The response of the tower under seismic action was assessed by carrying out a non-linear static (pushover) analysis. Its use for the seismic assessment of historical masonry structures has been proven to be a suitable approach and is widely documented in the literature [31–33]. In the current work, the pushover analyses were carried out using a load pattern based on horizontal forces proportional to the mass of the structure ("uniform pattern" according to EC8 [10]), which is a generally accepted procedure for complex masonry structures [31,34,35,36].

An incremental-iterative method is used assuming constant gravity loads and monotonically increasing the horizontal load. In this work, the regular Newton–Raphson iterative method was used in the non-linear phase. An energy-based convergence criterion (tolerance 1E-3) was considered. In addition, the Line Search algorithm and arc-length method were used as well to improve the convergence.

The seismic behavior of the building was evaluated according to the global horizontal axes, X and Y. Three pushover analyses were carried out in this phase: in positive X direction including the bell gable, in positive X direction discarding the bell gable, and in positive Y direction, also discarding the bell gable. Due to the symmetry of the tower, the analyses carried out discarding the bell gable in X and Y direction showed very similar results, both in terms of capacity curves (Fig. 7) and damage distribution. The capacity curve is expressed in terms of base shear factor (Load Factor, LF) versus displacement, LF being equal to the ratio between the sum of the horizontal forces and the total self-weight of the structure (dimensionless). For the reader's understanding, the self-weight of the structure is reported to be equal to 10797 T.
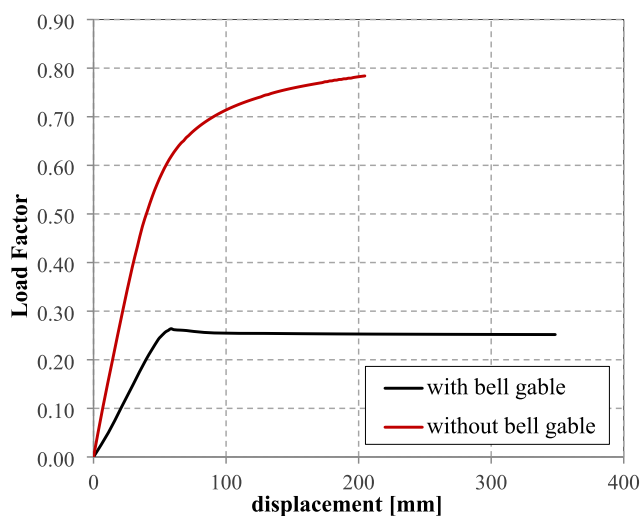

Fig. 7. Capacity curves for horizontal non-linear static analyses with and without the bell gable. Control point at the top of the tower.

The collapse of the bell gable due to the horizontal load applied in X direction is reached for a LF equal to 0.26 g, the corresponding damage distribution in terms of maximum principal strain (E1) is shown in Fig. 8 (a). The pushover analysis performed discarding the bell gable shows a high capacity of the structure in terms of Load Factor. The maximum LF is in fact equal to 0.8 g, corresponding to a maximum displacement of 200 mm. As it is visible in Fig. 8(b), at the end of the analysis the structure shows a global bending collapse mechanism, with damage appearing at the base of the tower in the facade that is orthogonal to the direction of the acting load and shear cracks in the plane of the walls that are parallel to the loading direction (results of the analysis in positive X direction are hereby presented). As shown in Fig. 8 (c), in the inner part of the tower the damage is mainly located in the walls bracing the corners of the structure and in the pillars and arches at Floor 2.

3. On-site inspection campaign and updating of the initial assumptions

In the second phase of the work, a comprehensive inspection and diagnosis campaign was carried out in order to increase the level of knowledge of the *Torre de la Vela*. This allowed to update the information obtained from the literature and check their accuracy. The experimental campaign included: geometrical survey carried out using laser scanning technique, sonic tests and dynamic identification tests. The latter two on site tests provided local information on material properties and global information on structural behavior.

3.1. Geometrical survey

The need for accurate geometric information regarding historical buildings, which are often irregular and characterized by numerous transformations, has been covered in the last years by the use of Laser Scanning Technology, which has proved to be an effective solution to perform the three-dimensional geometric reconstruction of historical masonry buildings. A high-resolution laser scanner survey was carried out in this work in order to obtain both the external and internal geometry of the *Torre de la Vela* in its current condition.

A point cloud was obtained from the laser scanner survey (Fig. 9), which was used to identify the main differences with respect to the geometry assumed in the first phase. The main differences found were:

1. inter-story heights, which have been updated, although the overall height of the tower initially assumed was confirmed;
2. configuration of Floor 1, which seems to be built directly by excavating the soil, creating the inner space of the dungeon. The survey has in fact shown the presence of a layer of soil with a height of 1.80 m below the space of Floor 1 (visible in Fig. 9 (c));
3. the South-East corner of Floor 1, i.e. a large part of the South and East facades, is completely buried (visible in Fig. 9 (b) at East façade). Since it was not possible to capture this configuration from the historical drawings and pictures, the whole Floor 1 was considered to be above ground in the first phase of the study.

The differences highlighted in points 2 and 3 cause a substantial change in the building-soil connection configuration, and this is likely to affect the structural response of the tower.

3.2. Sonic tests

Direct and indirect sonic tests were performed in order to obtain an estimation of the mechanical properties of the two main materials comprising the *Torre de la Vela*: rammed earth and brick masonry. Sonic impact tests also provide information regarding the internal condition of the tested structural element (such as presence of voids, masonry leaf detachment or cracks). This test is based on the generation of sonic pulses at several points of the structure using an instrumented hammer,
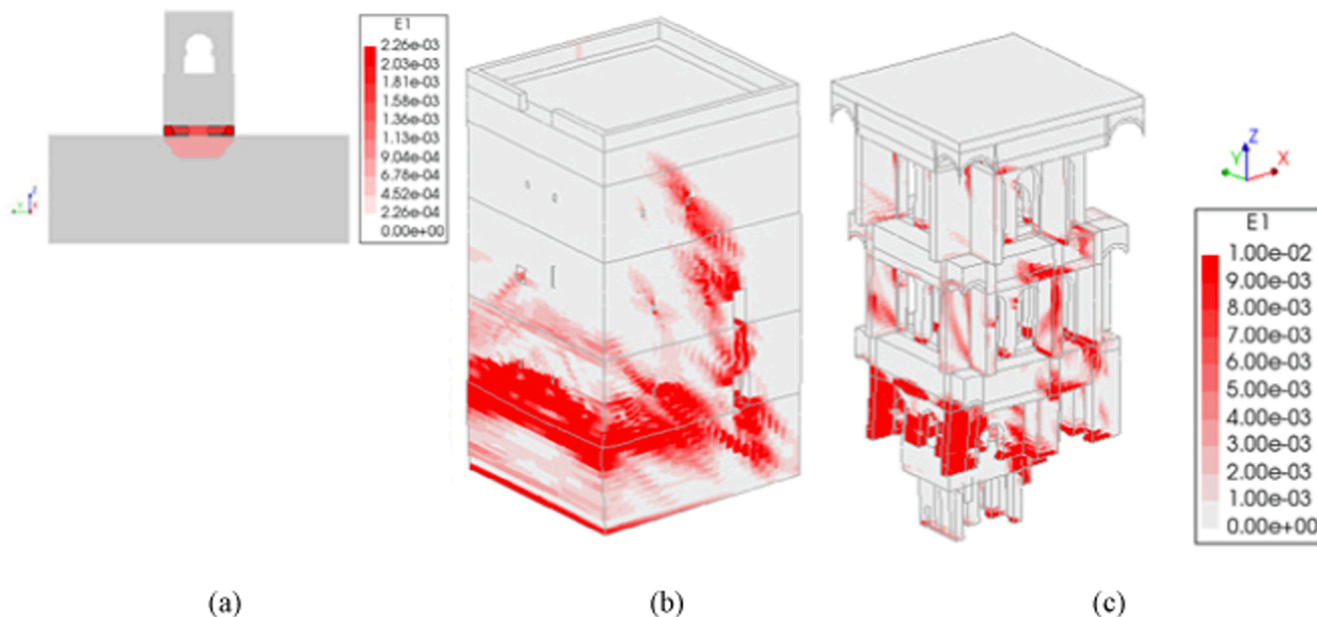
Fig. 8. Maximum principal strain distribution (a measure of cracking) at the end of the pushover analysis in X direction: (a) bell gable, (b) outer part of the tower, (c) inner part of the tower.
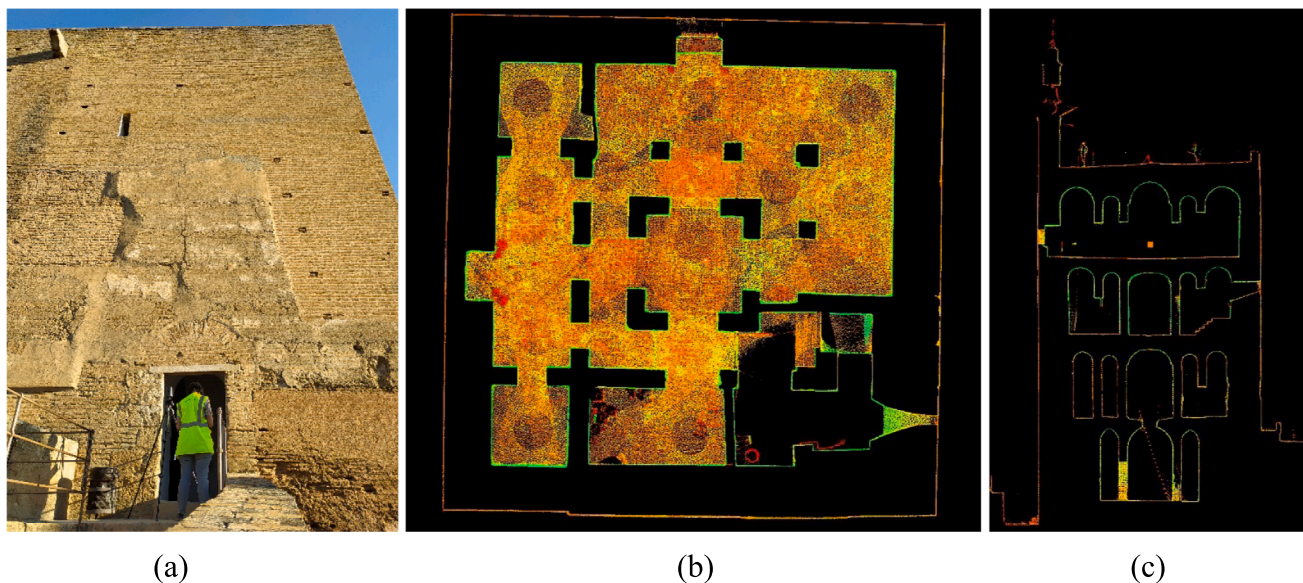

Fig. 9. (a) Geometric survey of the *Torre de la Vela* using a laser scanner; (b) fourth floor of the tower (point cloud); (c) South cross section (point cloud).

which propagate through the material and whose signal is then received by an accelerometer. The measurement of the velocity of propagation through the solid element of the generated P-waves and R-waves makes it also possible to obtain an estimation of the elastic mechanical properties of the materials, such as the Modulus of Elasticity (E), by correlating the velocities with material properties such as bulk density (ρ) and Poisson's ratio (ν).

Direct and indirect tests were conducted at different points of internal brick masonry elements located in Floor 2, 3 and 4. Indirect tests were also performed on the external masonry located in the South façade at Floor 2. As for the rammed earth, it was only possible to carry out indirect tests at certain points on the outer walls. 24 direct and 9 indirect tests were carried out on clay brick masonry elements, while 21 indirect tests were carried out on the rammed earth walls. Table 4 summarizes the results of sonic tests and points out the difference found

Table 4
Results of sonic tests and estimation of elastic properties.

		V_P [m/s]	V_R [m/s]	ρ [kg/m^3]	N [-]	E [MPa]
Brick masonry	Floors 2, 3 and 4	1220	620	1600	0.25	1,510
Rammed earth	Floor 1	2650	1400	2250	0.23	7,680
Rammed earth	Floor 2 and 4	1280	720		0.20	2,100

between floors for rammed earth.

As regards masonry, the average values of the P-wave and R-wave velocities are equal to 1220 m/s and 620 m/s and an average Poisson's

ratio value of 0.25 is obtained by correlating them. A bulk density equal to 1600 kg/m³ (assessed as shown in Section 2.3) was assumed to estimate the dynamic Elastic Modulus. The value of the final Elastic Modulus is considered to be equal to the 80% of the dynamic Elastic Modulus [37,38]. A value of 1,510 MPa was calculated, showing a good agreement with the one used for the literature-based analysis, assumed equal to 1,600 MPa.

As regards rammed earth, the experimental data shows a marked difference between the velocity values recorded on Floors 2 and 4, which are similar, and those recorded on Floor 1, which are significantly higher. In fact, for Floors 2 and 4, the average values of the P-wave and R-wave velocities are equal to 1280 m/s and 720 m/s, respectively, and an average Poisson's ratio equal to 0.20 is obtained. For Floor 1, the average values of the P-wave and R-wave velocities are equal to 2650 m/s and 1400 m/s, resulting in an average Poisson's ratio equal to 0.23. A density equal to 2250 kg/m³ was assumed to estimate the dynamic Elastic Modulus. While the results obtained from the tests on Floors 2 and 4 are in good agreement with the values found in literature (being the experimental value equal to 2,100 MPa and the literature one equal to 1,200 MPa), the values recorded on Floor 1 are clearly different, being the Elastic modulus equal to 7,680 MPa against 1,200 MPa assumed for the literature-based analysis. Eight tests were carried out on two different walls of Floor 1, and the coefficient of variation (CoV) is low (less than 10%), thus indicating reliable measures. This could be explained by considering that the external walls of Floor 1, a large part of which is buried, were not built but obtained by soil digging (as hypothesized for the entire floor), being themselves made of compacted original soil, thus resulting stiffer than the rammed earth employed at the other floors.

3.3. Dynamic identification tests

Dynamic identification tests were carried out in order to understand the dynamic characteristics of the structure and the connections with adjacent structures. Operational Modal Analysis (OMA) has been used to perform the dynamic identification test. The obtained dynamic properties of the building (i.e. natural frequencies and mode shapes) will be used to calibrate the numerical model. A multichannel high-resolution data acquisition system interfaced by accelerometers with 10 V/g

Fig. 10. Dynamic test setups.

sensitivity was utilized to conduct the test. The dynamic tests at the *Torre de la Vela* were carried out with four different setups, depicted in Fig. 10. The accelerometers were located at the mid-span of each perimeter wall and at the corners at Floor 4 (Setup 1 and 2) and Terrace (Setup 3 and 4), in order to catch the mode shapes of the tower. The setups were correlated by using a reference accelerometer (AC00 in Fig. 10) located at Floor 4. For each test setup, an acquisition time of 20 min with a 200 Hz sampling frequency was adopted.

The acquired dataset was then analyzed through the Operational Modal Analysis (OMA) software ARTeMIS Modal [39] by using Enhanced Frequency Domain Decomposition (EFDD) and Stochastic Subspace Identification – Principal Components (SSI-PC). Cross-validation of the results was conducted through the calculation of the Modal Assurance Criteria (MAC) [40] and the modes with a MAC higher than 0.60 were taken into account as reliable results (a MAC equal to 1 indicates a perfect match of the mode shapes obtained with the two methods). As a result, three modes of the structure were selected, whose frequencies range from 3 to 5 Hz. A summary of mode shapes and relative frequencies is provided in Fig. 11. The first two modes, characterized by translation in the orthogonal directions N-S and E-W, respectively, clearly show a global translational (or bending) dynamic behavior of the structure. It is noted that the frequencies and mode shapes of these two translational modes are quite different due to the boundary conditions of the tower. The third mode is torsional (or rotational), as it is often the case in towers.

4. Structural safety assessment of the *Torre de la Vela* considering data gathered on site

Collecting experimental data made it possible to update the initial linear-elastic properties and to consider realistic boundary conditions during the calibration process of the numerical model, discussed in Section 4.1. The same structural analyses, namely non-linear static analysis for vertical and horizontal loads, were then repeated on the updated model as shown in Section 4.2. The results obtained in this second phase of the work have been used to perform a seismic safety assessment of the tower. The differences between these results and those obtained in the first phase of the work are pointed out in Section 4.3 and allow to evaluate to what extent the use of *in situ* data can affect the numerical analysis, by reducing the uncertainty about the geometry, structural details and material data.

4.1. Model calibration based on experimental data

The numerical model validation involved the examination of the dynamic properties of the structure, namely the differences in main mode shapes and corresponding frequencies between the numerical (FE) and experimental (OMA) model. Calibration allows the difference between the experimental and numerical response to be minimized by changing relevant updating parameters until convergence is achieved. In particular, the Young's Modulus of the rammed earth was chosen as the parameter to be calibrated, as the analysis carried out on the literature-based model showed that the global response of the building mainly depends on the external walls. In addition, it was found appropriate to also consider an updating of the boundary conditions, in order to take into account the large buried parts at Floor 1 and to simulate the presence of intersecting structures, namely the wall at East façade and the staircase with the arched bridge leading to the main entrance of the *Torre de la Vela* at South façade (Fig. 12). In fact, the adjacent structures have an influence on the global stiffness of the tower and the mode shapes.

The calibration process started by considering the structure free from lateral constraints, and varying the Modulus of Elasticity in this configuration, starting from the experimental values identified after sonic tests for Floor 1 (E = 7,680 MPa) and for the other floors (E = 2,100 MPa). The two values were varied proportionally in order to keep

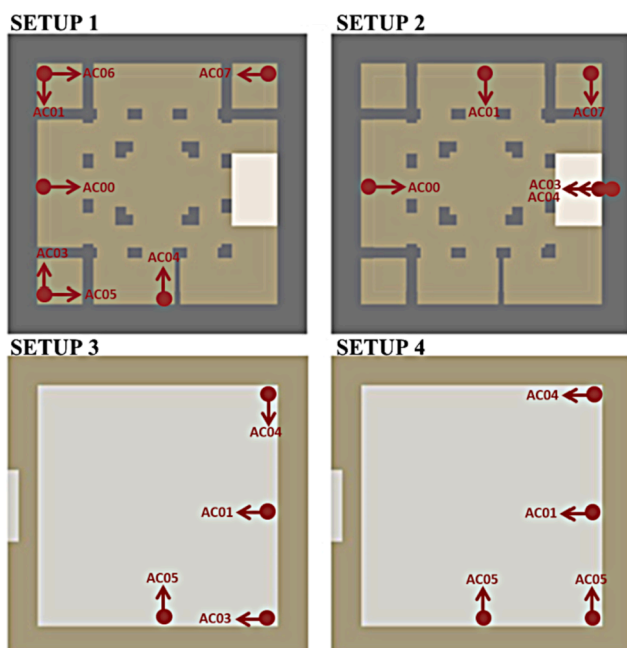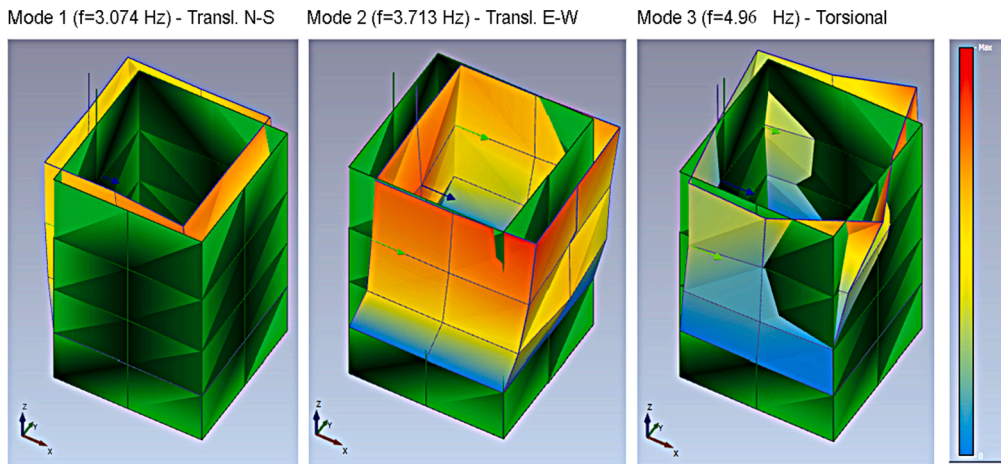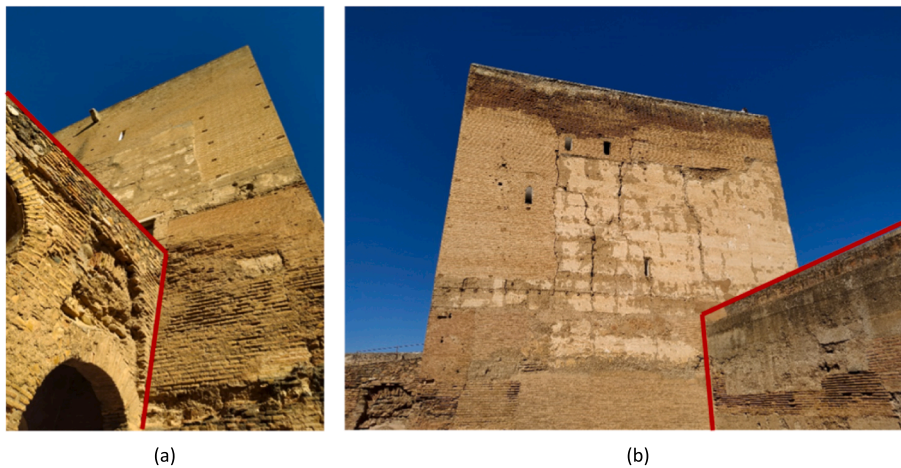**Fig. 11.** First three modes obtained by dynamic identification tests.

Fig. 12. Detail of the adjacent structures: (a) bridge at South façade; (b) wall at East façade.

constant the difference found by conducting sonic tests. To improve the efficiency of this procedure, the range of dynamic properties to be assessed was limited by only taking into account the following parameters: ratio between the first translation frequency in X direction (E-W) and the first torsional frequency; ratio between the first translation frequency in X direction and the first translation frequency in Y direction (N-S) [41,42]. Among the pairs of Young's Modulus values for which the average error between experimental and numerical frequencies was less than 10%, the one showing the minimum error in terms of the above-mentioned ratios was selected. The final values of the Young's Modulus to be considered for the updating of the numerical model are E = 5,900 MPa for the Floor 1 and E = 1,100 MPa for the other floors.

Once these values were set, the lateral restraints were addressed. The configuration that best matched the experimental mode shapes was found to be the one considering a rigid connection between the East façade and the intersecting wall in the direction orthogonal to the façade (obtained by restricting the displacement in that direction) and no connection between the South façade and the intersecting bridge. This suggests a separation between the tower and the bridge. The updated boundary conditions are shown in Fig. 13 (a), in comparison with the
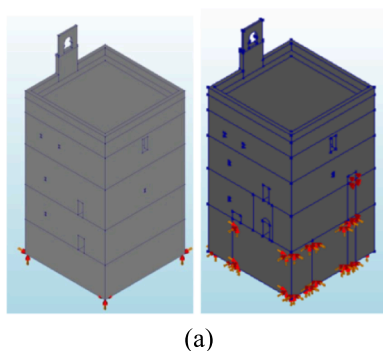
DYNAMIC PROPERTIES

Mode	Mode Shape	Numerical Frequency [Hz]	Experimental Frequency [Hz]	error [%]
1	transl -y	3.25	3.07	5.87%
2	transl -x	3.54	3.71	4.62 %
3	torsion	5.20	4.96	4.80%
			AVG	**5.10%**

(a)   (b)

Fig. 13. (a) Comparison between the boundary conditions considered in the preliminary (left) and final (right) model; (b) comparison between numerical and experimental mode shapes after model calibration.

ones considered for the preliminary numerical model. After the calibration process, the numerical model was able to reproduce the first three experimental modes with an average error of the frequency values equal to 5%, as shown in Fig. 13 (b). A further validation was carried out by comparing the mode shapes of the numerical and experimental model through MAC (Modal Assurance Criterion) values. The calibrated model of the *Torre de la Vela* resulted in an average MAC value for the three modes equal to 0.97, showing a successful validation if compared with a MAC equal to 1, which indicates a perfect correlation.

4.2. Structural behavior evaluation

4.2.1. Vertical non-linear static analysis

Non-linear static analysis for vertical loads was carried out again by increasing the load up to a value equal to the double of the building self-weight. As for the literature-based model, the global behavior of the structure is linear for a Load Factor equal to 2. As expected, the obtained values in terms of stresses and strains are low and vary in a small range.

Fig. 14 shows the maximum principal strain (E1) distribution (a measure of cracking) for a Load Factor equal to 1. The results are plotted above peak tensile strain for both rammed earth (5.08E-5) in Fig. 14 (a) and masonry (1.25E-4) in Fig. 14 (b). Cracking distribution is similar to that obtained for the preliminary model, with a concentration in the pillars at Floor 2. In this case, damage is also observed in the base of the corner walls at Floor 3, not present in the literature-based model. In addition, cracking is also observed in the external rammed earth walls at Floor 1, due to the variation of lateral restraint with respect to the preliminary model. On the other hand, crushing distribution is the same as that observed in the preliminary model, so the results are not repeated here.

4.2.2. Horizontal non-linear static analysis

Pushover analyses were repeated using the calibrated model. In this case, the results of the analyses in X and Y directions are clearly different due to the updated boundary conditions, the presence of which leads to the behavior of the structure no longer being symmetrical. Therefore, four pushover analyses were performed: positive X direction (+X) including the bell gable, positive X direction (+X) discarding the bell gable, negative X direction (-X) discarding the bell gable and positive Y direction (+Y). The analysis in the negative Y (-Y) direction was discarded because, given the boundary conditions, the structure would

have shown a certainly higher capacity than in the positive +Y direction. Fig. 15 shows the results of the pushover analyses in terms of capacity curves using a point at the top of the tower as a control node to plot the displacements.

The structural response of the building considering the presence of the bell gable can be observed through the analysis in the +X direction. The collapse of the bell gable due to the horizontal load applied in the +X direction is reached for a LF equal to 0.28 g. Cracking distribution at the end of the analysis is shown in Fig. 16 (a) in terms of maximum principal strain (E1).

Neglecting the bell gable, the tower shows its maximum horizontal capacity in the +X direction. The behavior of the tower is linear up to approximately 0.8 g. The maximum achieved load in this direction corresponds to a LF of 1.60 g. This result is due to the presence of boundary conditions acting in the opposite direction and preventing the bending collapse mechanism (buried parts at Floor 1 and the presence of the intersecting wall at East façade). In the +Y direction, the structural behavior of the tower is linear up to 0.55 g, the maximum horizontal capacity is equal to 1.10 g. The structure shows its lowest seismic capacity, equal to 0.90 g, in the -X direction.

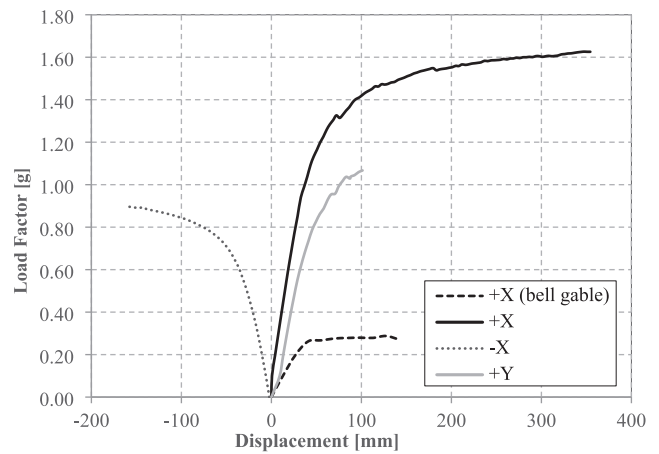The results of the analyses performed in the +X and +Y directions is

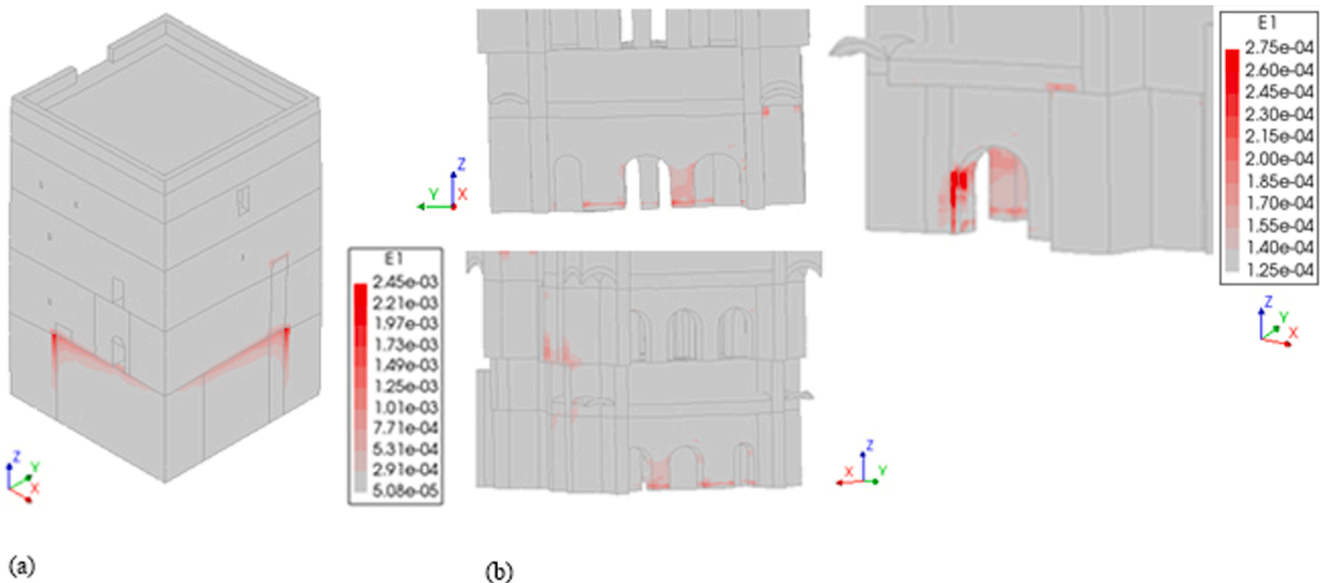Fig. 15. Capacity curves for pushover analyses.

(a)   (b)

Fig. 14. (a) Maximum principal strain distribution in rammed earth walls above peak tensile strain (5.08E−5); (b) maximum principal strain distribution in masonry walls above peak tensile strain (1.25E−4).
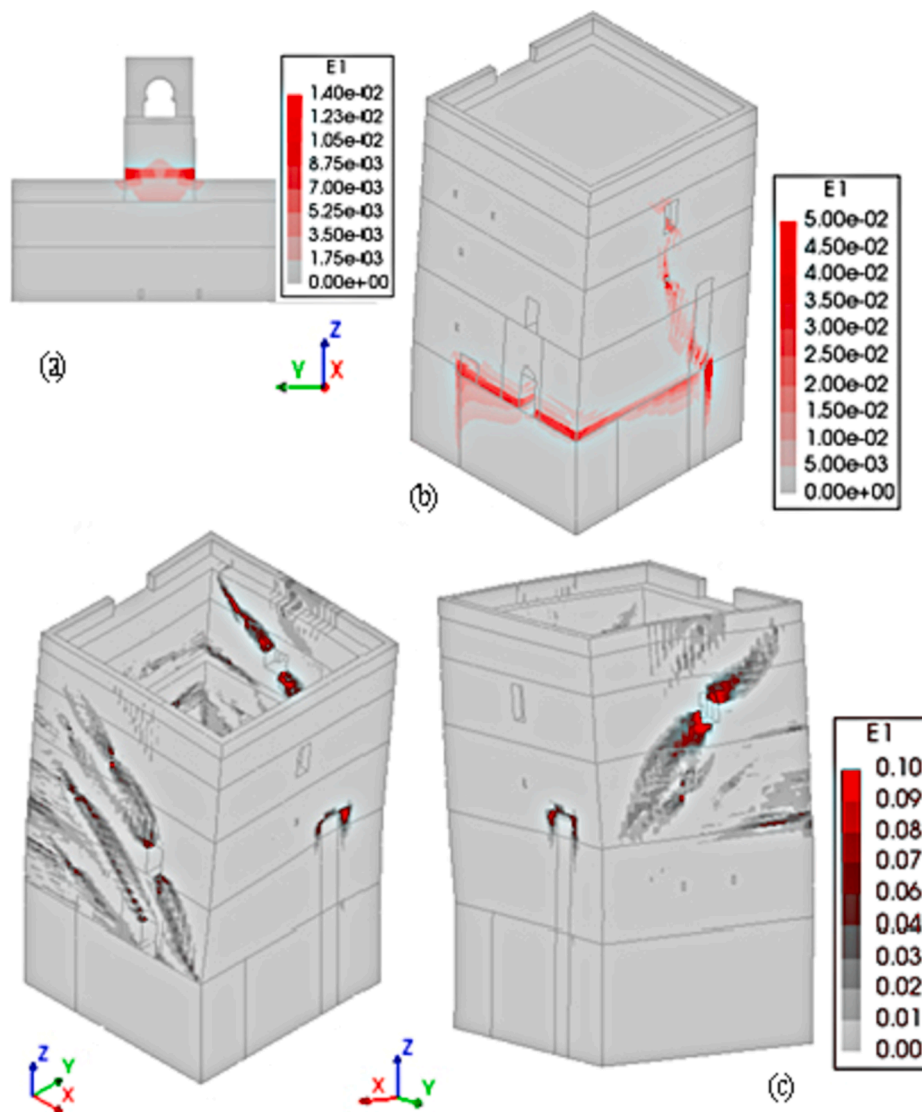
Fig. 16. Damage distribution in external walls in terms of maximum principal strain (E1) at the end of the pushover analyses: (a) +X with bell gable, (b) +Y, (c) +X.

provided in Fig. 16 (b), (c) in terms of damage, while a more comprehensive overview of the results of the –X direction analysis is given in Fig. 17. Damage distribution is again shown in terms of maximum principal strain (E1). As visible in Fig. 16, in both directions the structure shows a global bending collapse mechanism. In the +Y direction analysis (Fig. 16 (b)), the damage is mainly located at the connection between Floor 1 and Floor 2, corresponding to the buried areas. The damage pattern is characterized by shear cracks in the plane of the East facade, that is parallel to the loading direction. In the +X direction analysis, the damage pattern is characterized by shear cracks in the plane of the walls parallel to the load direction, mostly occurring at openings. The presence of the intersecting wall at East façade clearly counteracts the global rotation of the tower and damage is prevented in the lower floors.

The evolution of the damage distribution during the –X direction analysis is shown in Fig. 17. For a LF equal to 0.60 g (Fig. 17 (a)), the global behavior of the tower is still basically linear, with limited damage appearing in the inner structural elements at the base of the pillars. In the non-linear phase of the analysis (Fig. 17 (b)), shear cracks appear in the plane of the inner corner walls parallel to the loading direction, mainly at Floor 2 and 3. In the outer walls the damage is limited to the connection between Floor 1 and Floor 2 and with the intersecting wall at the East façade. At the end of the analysis (Fig. 17 (c)), the inner damage

pattern is characterized by widespread shear cracks at all floors of the tower in the South-East area. In the outer walls, the existing damage at the connections increases.

4.2.3. Seismic safety assessment

The seismic vulnerability of the tower is assessed for the most vulnerable direction detected in the pushover analyses in terms of force capacity (negative X direction). It is noted that the results from the analysis including the gable wall were disregarded because the seismic safety assessment aimed to analyze the global behavior of the structure and not the local failure of the gable wall. The assessment is performed following the N2 method [43], which is adopted on many structural codes, such as Eurocode 8, Annex B of EN 1998-1 [10]. The procedure consists of comparing the seismic demand or target displacement (d_t), expressed in terms of spectral displacement of an equivalent Single Degree Of Freedom (SDOF) system, with the displacement capacity of the structure, expressed in terms of an idealized capacity curve of the SDOF system. This method is adopted for the seismic assessment of several historical masonry structures [44–48] and is here applied for an emblematic earthen structure of the Alhambra, the *Torre de la Vela*.

The elastic spectrum is defined according to the Eurocode 8. It is noted that the pushover analyses already revealed that the tower with its massive earthen walls has a significant capacity against horizontal
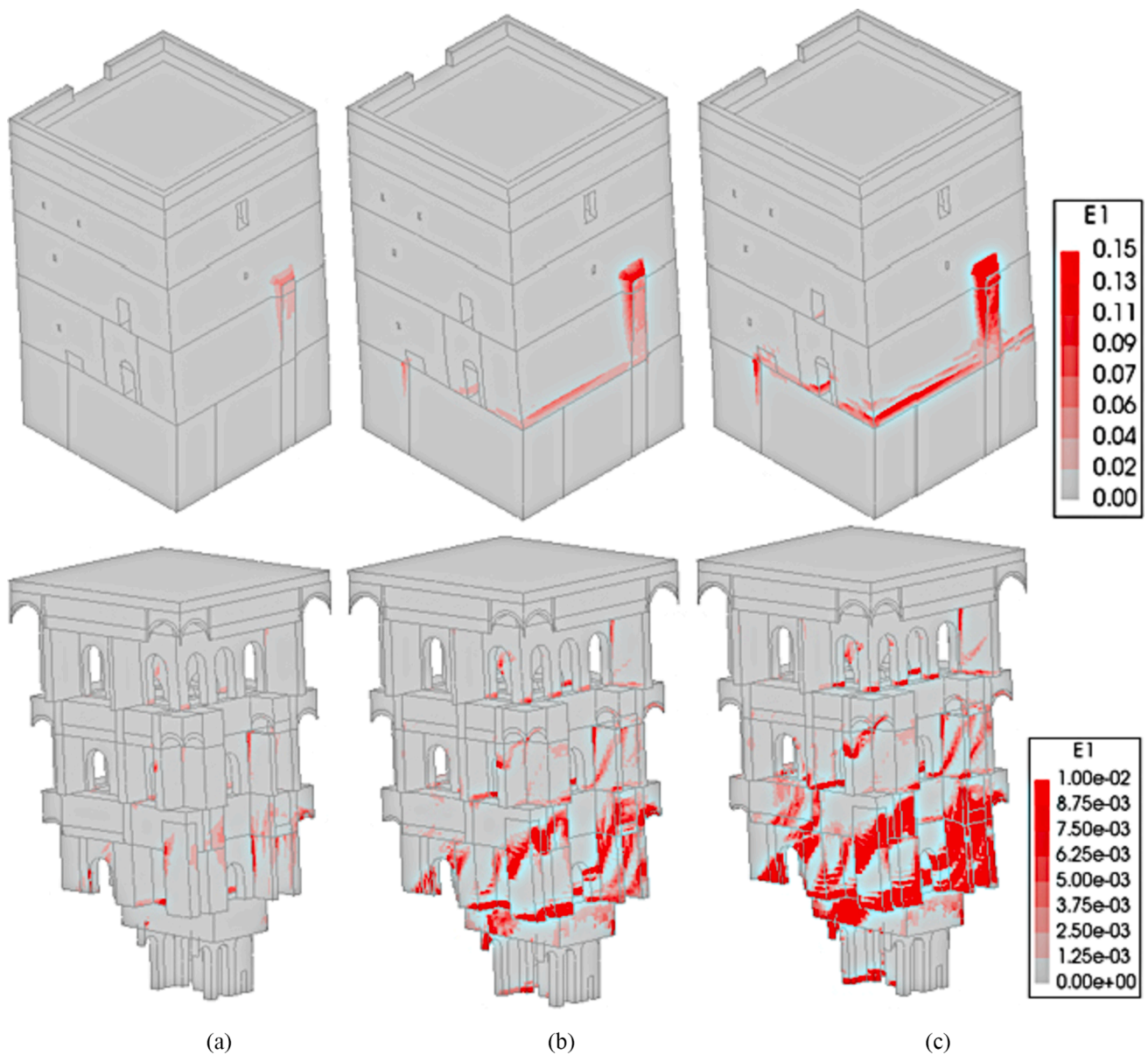
Fig. 17. Damage distribution in terms of maximum principal strain (E1) at different steps of the analysis in the –X direction: (a) LF = 0.60, (b) LF = 0.80, (c) LF = 0.90.

loading, reaching a maximum value of 0.90 g in -X direction. Therefore, the parameters used to obtain the response spectrum were estimated for a 2475-year mean return period earthquake (2% chance of exceedance in 50-year) instead of the common 500-year mean return period earthquake established in the Spanish standard [49]. Additionally, an importance factor (γ_i) of 1.4 was assumed in order to account for the high cultural significance of the building [10]. As a result of applying the modifying factors, the Peak Ground Acceleration, originally established as 0.23 g by the Spanish code for Granada (500-year mean return period), is 0.62 g. A ground type D (as defined by Eurocode 8) is chosen as representative of local conditions and the Type 2 (near-field) type of spectrum is considered (per indications of the NCSE-02 Spanish Norm).

The pushover curve obtained from the numerical analysis (Fig. 15 -X direction) is transformed into the bilinear idealized capacity curve of an equivalent SDOF system following the procedure defined in Annex B of EN 1998-1 [10]. Once the equivalent bilinear SDOF curve and the response spectrum has been estimated, the period T^* of the idealized SDOF system and the target displacement (d_t) for the Multiple Degree of Freedom System (MDOF) can be computed. Fig. 18 (a) shows the results

of the calculation of T^* and the target displacement for the SDOF system, following the N2 procedure, and Fig. 18 (b) shows its transformation into the target displacement (d_t) for the MDOF and the comparison with the pushover curve from the numerical analysis.

The displacement-based verification shown in Fig. 18 confirm the significant capacity of the structure against horizontal loading. The target displacement imposed by the earthquake considered is lower than the ultimate displacement of the of the idealized capacity curve (marked in red in Fig. 18 (b)). Further verifications can be carried out by comparing the target displacement with damage limit states. In this work, the limit states proposed by Lagomarsino and Giovinazzi (2006) [50] are adopted, which consider four limit states as a function of the yield displacement d_y and the ultimate displacement d_u of the idealized bilinear capacity curve. Note that the yield displacement corresponds to the displacement required for the structure to reach the yield maximum strength in the idealized bilinear curve. The four limit states are depicted graphically in Fig. 18 (b) and summarized in Table 5.

According to Table 5, the target displacement imposed by the earthquake evaluated would cause significant damage to the structure,
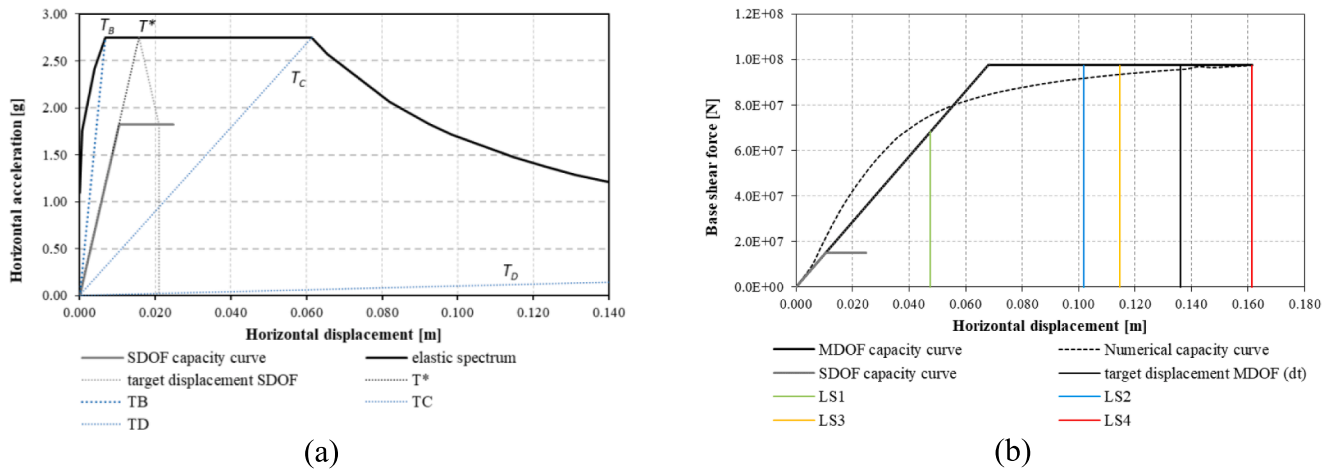
Fig. 18. (a) Determination of the target displacement for the equivalent SDOF system (N2 method); and (b) target displacement for the MDOF system and comparison with damage limit states.

Table 5
Definition of limit states by Lagomarsino and Giovinazzi (2006) [50].

Damage Limit State (LS)	Description	Performance Level	Displacement threshold
LS1	Slight	Fully operational	$0.7d_y$
LS2	Moderate	Operational	$1.5d_y$
LS3	Heavy	Life safe	$0.5(d_y + d_u)$
LS4	Complete	Near collapse	d_u

exceeding LS3. Therefore, despite the overall significant capacity of the structure, it is expected that the same suffers important damage due to the earthquake under consideration (2475-year mean return period). It is also noted that during the on-site campaign, a damage survey was carried out, identifying that the tower already presents significant damage (extensive cracking in exterior walls and vaults), which may also increase the vulnerability of the structure to future earthquakes.

4.3. Comparison with the preliminary model

A comparison of the seismic response of the tower using the preliminary and calibrated models is shown in Fig. 19, in terms of capacity
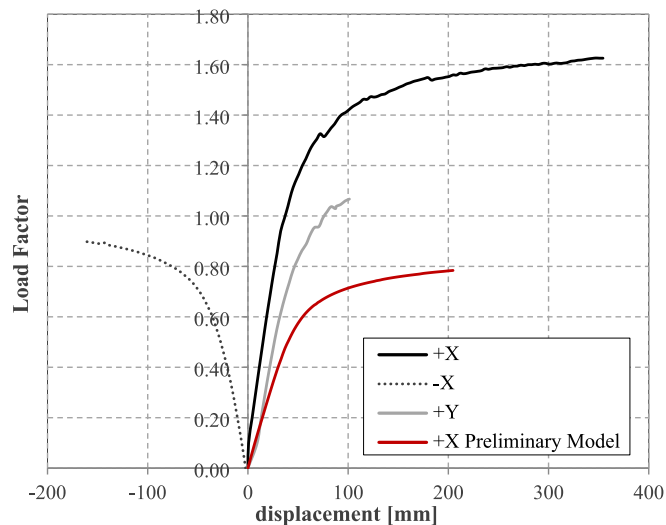

Fig. 19. Comparison of capacity curves obtained with the preliminary and final calibrated models.

curves. It can be observed that the maximum horizontal capacity in terms of force for the +X direction is almost doubled in the calibrated model. As expected, the model is stiffer due to the increased Modulus of Elasticity used for Floor 1 and the boundary conditions, in particular due to the addition of the wall intersecting the East façade as a lateral restraint. The analysis in the -X direction shows a lower horizontal capacity due to the absence of lateral constraint. The updated boundary conditions (presence of built elements intersecting the tower and buried parts at Floor 1) caused the loss of the symmetrical behavior exhibited by the preliminary model.

The structure still shows a global bending collapse mechanism, but the most important cracks that lead to the rotation of the tower now appear at the interface between the Floor 1 and the upper floors. In-plane shear cracks on the walls and pillars that are parallel to the acting load direction are still characterizing the damage pattern in the inner structural elements of the towers. They are also present in the outer walls, except for the -X direction analysis, in which the damage is concentrated at the connections between Floor 1 and Floor 2 and mostly between East façade and the intersecting wall considered as lateral restraint, illustrating the separation between both elements.

The difference in stiffness between the floors has a significant influence on the structural behavior of the tower, as well as the actual boundary conditions, illustrating the importance of the experimental on-site works to prepare a numerical model that is more similar to the real building configuration and allows to have greater confidence on the results.

5. Conclusion

A 3D Finite Element model was prepared and validated to perform a safety assessment of the *Torre de la Vela* in the *Alhambra* of Granada (Spain). Structural analysis of historic buildings is essential for this purpose and requires on site data acquisition in order to increase the level of knowledge of the building and to prepare a reliable numerical model. This phase includes historical, structural and construction process investigations, geometrical survey of the structure, field research and material testing.

In the first phase of this study, preliminary numerical analyses were carried out to assess the structural behavior of the building, based entirely on a literature review, with limited information on the geometry, mechanical properties of the materials and construction details, given the pandemic situation. In the second phase, an extensive inspection and diagnosis campaign allowed to characterize the main structural aspects necessary to evaluate the state of conservation of the building and calibrate the numerical model. The final numerical model

was more reliable and better represented the actual conditions of the building. Since the *Alhambra* is located in the area with the highest seismic hazard in Spain, the seismic safety of the tower was specifically investigated. The results of the seismic analysis showed that one direction is the most vulnerable because of lack of lateral restraint, which is provided by both massive buried areas at the basement of the tower and adjacent structures in the other orthogonal directions.

The displacement-based assessment carried out following indications of current codes confirmed that the structure has a significant capacity under earthquake loading, mainly due to the massive earthen walls and geometric proportions. Nevertheless, the assessment reveals that the structure is expected to suffer important damage due to the earthquake under consideration (2475-year mean return period). Besides, existing damage in the structure (extensive cracking in walls and vaults) contribute to the overall seismic vulnerability of the structure.

The work also shows how the structural behavior of the two numerical models (preliminary and calibrated) is significantly different and to what extent the information obtained from a literature study concerning geometry and material properties was modified as a result of the experimental campaign. The results highlight the importance of *in-situ* experimental testing for a reliable structural analysis of historical buildings.

CRediT authorship contribution statement

Annalaura Vuoto: Conceptualization, Methodology, Formal analysis, Investigation, Resources, Data curation, Writing – original draft, Writing – review & editing, Visualization. **Javier Ortega:** Conceptualization, Methodology, Formal analysis, Investigation, Resources, Data curation, Writing – original draft, Writing – review & editing, Visualization, Supervision, Project administration, Funding acquisition. **Paulo B. Lourenço:** Conceptualization, Methodology, Resources, Writing – review & editing, Supervision, Project administration, Funding acquisition. **Francisco Javier Suárez:** Investigation, Resources, Data curation, Writing – original draft, Writing – review & editing, Project administration, Funding acquisition. **Antonieta Claudia Núñez:** Investigation, Resources, Data curation, Writing – review & editing.

Declaration of Competing Interest

The authors declare that they have no known competing financial interests or personal relationships that could have appeared to influence the work reported in this paper.

Acknowledgments

References

[1] International Charter for the conservation and restoration of monuments and sites (The Venice Charter). ICOMOS - International Council of Monuments and Sites, Venice; 1964.

[2] European Charter of the Architectural Heritage 1975. ICOMOS - International Council of Monuments and Sites, Amsterdam; 1975.

[3] Gallego Burín A. GRANADA, Guía artística e histórica de la ciudad, 1987th ed. Granada: COMARES; 1987.

[4] Barrios Rozúa J. Alhambra romántica: los comienzos de la restauración arquitectónica en España, Granada. Granada: Universidad de Granada; 2016.

[5] Calatrava Escobar J. La Alhambra y el orientalismo arquitectónico. El Manifiesto de la Alhambra 50 años despúes. Granada: Consejería de cultura Junta de Andalucía; 2003.

[6] Calatrava Escobar J. El arte hispanomusulmán y las exposiciones universales: de Owen Jones a Leopoldo Torres Balbás. AWRAQ. Rev. análisis y Pensam. sobre el mundo árabe e islámico, no. 11, pp. 7–31; 2015.

[7] Manzano R. La Alhambra. ANAYA: El universo mágico de la Granada Islámica; 1992.

[8] Gòmez-Moreno Calera JM. Estructuras defensivas de la Alhambra, I. Cuestiones Generales. pp. 125–154; 2002.

[9] "Torre de la Vela," andaltura.com. [Online]. Available: http://www.andaltura. com/andalucia/la-alhambra-y-el-generalife/torres-de-la-alhambra/torre-de-la-vela . [accessed: 17-Apr-2020].

[10] European Committee for Standardisation. EN 1998-1 (Eurocode 8). Design of structures for earthquake resistance, Part 1 General rules seismic actions and rules for buildings. Brussels, Belgium; 2003.

[11] Justo JL, Azañón JM, Azor A, Saura J, Durand P, Villalobos M, et al. Neotectonics and slope stabilization at the Alhambra, Granada, Spain. Eng Geol 2008;100(3-4): 101–19.

[12] Gómez-Moreno Martinez M. Granada en el siglo XIII. In: Monumentos arquitectóncos de España, 2nd ed., Granada; 1907.

[13] López Bueno M, Torres Balbás L. Torre de la Vela. Patronato de la Alhambra y Generalife 1923.

[14] Pavón Maldonado B. La Alcazaba de la Alhambra. Cuad La Alhambra 1971;7:3–34.

[15] Villegas Cerredo D. "Análisis estructural del patrimonio histórico. Torre del Homenaje de la Alhambra", Master de Estructuras -. Universidad de Granada; 2012.

[16] de la Torre López MJ, Sebastián PE, Rodríguez GJ. A study of the wall material in the alhambra (Granada, Spain). Cem Concr Res 1996;26(6):825–39.

[17] González Limón T, Casas Gómez A. Estudio de los materiales y de las fábricas de la Torre de Comares de la Alhambra. Cuad. La Alhambra; 1997.

[18] González Limón T, Casas Gómez A. Estudio de los materiales y de las fábricas de la Torre de Comares de la Alhambra. Cuad. La Alhambra, no. 33, pp. 95–104; 1997.

[19] Ruano EB. Tópicos y realidades de la Edad Media. Real Academia de la Historia 2000.

[20] "Torre de la Vela,". *Alhambra-patronato*. [Online]. Available: https://www.alhambra-patronato.es/edificios-lugares/torre-de-la-vela [accessed: 17-Apr-2020].

[21] Borrás G. "La Alhambra actual y la Alhambra nazarí," *artehistoria.com*. [Online]. Available: https://www.artehistoria.com/es/contexto/la-alhambra-actual-y-la -alhambra-nazarí. [accessed: 09-Apr-2020].

[22] Molina Lòpez E. El emirato nazarí de Granada. El último bastión del Islam andalusí. Andalucía en la Historia, Univ. de Granada; 2013.

[23] DIANA FEA BV. Diana User's Manual, Release 10.4. Delft: DIANA FEA BV; 2020.

[24] Lourenço Paulo B, Pereira João M. Recommendations for Advanced Modeling; 2018.

[25] Circolare 21 gennaio 2019 n.7 "Istruzioni per l'applicazione dell'«Aggiornamento delle "Norme tecniche per le costruzioni"» di cui al decreto ministeriale 17 gennaio 2018″ (in Italian), vol. 35. Italy, 2019, p. 257.

[26] NTC 2018. Norme Tecniche per le Costruzioni. Ministero delle Infrastrutture e dei Trasporti. (in Italian). Italy; 2018.

[27] Ortega J, Vasconcelos G, Rodrigues H, Correia M. Assessment of the efficiency of traditional earthquake resistant techniques for vernacular architecture. Eng Struct 2018;173(February):1–27.

[28] Lourenço P. Recent advances in masonry structures: micromodelling and homogenization. In: Multiscale modeling in solid mechanics: computational approaches., Imperial College Press; 2009, pp. 280–300.

[29] Selby RG, Vecchio FJ. A constitutive model for analysis of reinforced concrete solids. Can J Civ Eng 1997;24(3):460–70.

[30] Vecchio FJ, Collins MP. The modified compression-field theory for Reinforced Concrete Elements subjected to shear. ACI J 1986;83–22:219–31.

[31] Lourenço Paulo B, Mendes Nuno, Ramos Luís F, Oliveira Daniel V. Analysis of Masonry Structures Without Box Behavior. Int J Archit Herit 2011;5(4-5):369–82.

[32] Peña F, Lourenço PB, Mendes N, Oliveira DV. Numerical models for the seismic assessment of an old masonry tower. Eng Struct 2010;32:1466–78.

[33] O'Hearne N, Mendes N, Lourenço PB. Seismic analysis of the San Sebastian Basilica (Philippines). In: 40th IABSE Symposium: Tomorrow's Megastructures; 2018.

[34] Lagomarsino S, Penna A, Galasco A, Cattari S. TREMURI program: An equivalent frame model for the nonlinear seismic analysis of masonry buildings. Eng Struct Nov. 2013;56:1787–99.

[35] Endo Y, Pelà L, Roca P. Review of Different Pushover Analysis Methods Applied to Masonry Buildings and Comparison with Nonlinear Dynamic Analysis. J Earthq Eng 2017;21(8):1234–55.

[36] Lagomarsino S, Cattari S, Lagomarsino S, Cattari S. PERPETUATE guidelines for seismic performance-based assessment of cultural heritage masonry structures. vol. 13, pp. 13–47; 2015.

[37] D'Ambrosi A, Mariani V, Mezzi M. Seismic assessment of a historic masonry tower with nonlinear static and dynamic analyses tuned on ambient vibration tests. Eng Struct 2012;36:210–9.

[38] Ripepe M, Coli M, Lacanna G, Marchetti E, Cristofaro MT, De Stefano M. Dynamic response of the Giotto's Bell-Tower, Firenze, Italy. Eng Geol 2014;8:323–7.

[39] ARTeMIS Modal Users' Manual; 2014.

[40] Ewins, D. Modal Testing: Theory, Practice and Application, 2nd editio. Baldock-Hertfordshire, UK: Research Studies Press LTD; 2000.

[41] Ferraioli M, Miccoli L, Abruzzese D, Mandara A. Dynamic characterization of a historic bell-tower using a sensitivity-based technique for model tuning. J Civ Struct Heal Monit 2018;8:253–69.

[42] Pavlovic Milorad, Trevisani Sebastiano, Cecchi Antonella. A Procedure for the Structural Identification of Masonry Towers. J Nondestruct Eval 2019;38(2). https://doi.org/10.1007/s10921-019-0575-8.

[43] Fajfar Peter. Capacity spectrum method based on inelastic demand spectra. Earthq Eng Struct Dyn 1999;28(9):979–93.

[44] Saloustros Savvas, Pelà Luca, Contrafatto Francesca R, Roca Pere, Petromichelakis Ioannis. Analytical Derivation of Seismic Fragility Curves for Historical Masonry Structures Based on Stochastic Analysis of Uncertain Material Parameters. Int J Archit Herit 2019;13(7):1142–64.

[45] Acito Maurizio, Bocciarelli Massimiliano, Chesi Claudio, Milani Gabriele. Collapse of the clock tower in Finale Emilia after the May 2012 Emilia Romagna earthquake sequence: Numerical insight. Eng Struct 2014;72:70–91.

[46] Castellazzi Giovanni, D'Altri Antonio Maria, de Miranda Stefano, Ubertini Francesco. An innovative numerical modeling strategy for the structural analysis of historical monumental buildings. Eng Struct 2017;132:229–48.

[47] Simões A, Milošević J, Meireles H, Bento R, Cattari S, Lagomarsino S. Fragility curves for old masonry building types in Lisbon. Bull Earthq Eng 2015;13: 3083–105.

[48] Cantagallo Cristina, Spacone Enrico, Perrucci Daniele, Liguori Nicola, Verazzo Clara. A multilevel approach for the cultural heritage vulnerability and strengthening: Application to the melfi castle. Buildings Sep. 2020;10(9):158. https://doi.org/10.3390/buildings10090158.

[49] Centro de Publicaciones Secretaria General Técnica Ministerio de Fomento, Norma de Construcción Sismorresistente: Parte general y edificación (NCSE-02); 2009.

[50] Lagomarsino Sergio, Giovinazzi Sonia. Macroseismic and mechanical models for the vulnerability and damage assessment of current buildings. Bull Earthq Eng 2006;4(4):415–43.